J|A|C|S
ARTICLES
Published on Web 08/19/2006

Isolation, Structure, and Absolute Stereochemistry of Platensimycin, A Broad Spectrum Antibiotic Discovered Using an Antisense Differential Sensitivity Strategy

Sheo B. Singh,*,† Hiranthi Jayasuriya,† John G. Ondeyka,† Kithsiri B. Herath,† Chaowei Zhang,† Deborah L. Zink,† Nancy N. Tsou,† Richard G. Ball,† Angela Basilio,‡ Olga Genilloud,‡ Maria Teresa Diez,‡ Francisca Vicente,‡ Fernando Pelaez,‡ Katherine Young,† and Jun Wang†

Contribution from Merck Research Laboratories, P.O. Box 2000, Rahway, New Jersey 07065, and CIBE, Merck Sharp & Dohme de Espana, S. A. Josefa Valcárcel, Madrid, Spain

Received April 10, 2006; E-mail: sheo_singh@merck.com

Abstract: Fatty acids are essential for survival of bacteria and are synthesized by a series of enzymes including the elongation enzymes, β-ketoacyl acyl carrier protein synthase I/II (FabF/B). Inhibition of fatty acid synthesis is one of the new targets for the discovery and development of antibacterial agents. Platensimycin (**1a**) is a novel broad spectrum Gram-positive antibiotic produced by *Streptomyces platensis*. It was discovered by target-based whole-cell screening strategy using antisense differential sensitivity assay. It inhibits bacterial growth by selectively inhibiting condensing enzyme FabF of the fatty acid synthesis pathway and was isolated by a two-step process, a capture step followed by reversed-phase HPLC. The structure was elucidated by 2D NMR methods and confirmed by X-ray crystallographic analysis of a bromo derivative. It was determined that potential reactivity of the enone moiety does not play a key role in the biological activity of platensimycin. However, cyclohexenone ring conformation renders for the stronger binding interaction with the enzyme. The isolation, structure elucidation, derivatization, and biological activity of 6,7-dihydroplatensimycin are described.

Introduction

Emergence of bacterial resistance to all known classes of antibiotics is of significant cause for concern, and continued discovery of new antibiotics with novel modes of action is critical to overcoming the resistant organism.[1] Fatty acids are required for bacterial survival, and their biosynthesis is catalyzed by a highly conserved condensing enzyme, FabF.[2] This enzyme elongates the growing fatty acid chain by adding acetate units generating a β-ketoacyl substrate. This substrate enters into a cycle and undergoes various enzymatic reductions and, in an iterative process, produces the desired fatty acids.[3] The FabF target has been a subject of studies for more than 20 years, and two classes of inhibitors have been reported. These are cerulenin[4] and thiolactomycin.[5] However, all are very poor inhibitors (IC_{50} ranges 1.5−13 μg/mL) with poor antibacterial activity (*Staphylococcus aureus* MIC 64 μg/mL).[6] Potent inhibitors of this enzyme are expected to afford antibiotics with no cross-resistance to existing drugs.

Screening of natural product extracts using the newly described[7] antisense differential sensitivity whole-cell two-plate agar diffusion assays and bioassay-guided fractionation of an extract produced by fermentations of *Streptomyces platensis*, recovered from soil samples collected in South Africa and Spain, led to the isolation of platensimycin (**1a**, Figure 1). This novel natural product selectively inhibited *S. aureus* FabF and *Escherichia coli* FabF/B enzymes with IC_{50} values of 48 and 160 nM and was a weak inhibitor of *S. aureus* FabH (IC_{50} 67 μM). This compound inhibited phospholipid synthesis (IC_{50} 0.1 μg/ mL), exhibited MIC values of 0.1−1 μg/mL against MRSA and VRE, and provided more than four log reductions in cfu counts of *S. aureus* in a mouse model at 100 μg/h continuous infusion for 24 h without showing any overt toxicity.[8] Mechanistically, it exerts its activity by a novel mode of action that

† Merck Research Laboratories.
‡ CIBE.

(1) (a) Walsh, C. T. *Nat. Rev. Microbiol.* **2003**, *1*, 65−70. (b) Singh, S. B.; Barrett, J. F. *Biochem. Pharmacol.* **2006**, *71*, 1006−1015.
(2) (a) Revill, W. P.; Bibb, M. J.; Scheu, A.-K.; Kieser, H. J.; Hopwood, D. A. *J. Bacteriol.* **2001**, *183*, 3526−3530. (b) Lai, C.-Y.; Cronan, J. E. *J. Biol. Chem.* **2003**, *278*, 51494−51503. (c) Tsay, J. T.; Rock, C. O.; Jackowski, S. *J. Bacteriol.* **1992**, *174*, 508−513. (d) Schujman, G. E.; Choi, K.-H.; Altabe, S.; Rock, C. O.; de Mendoza, D. *J. Bacteriol.* **2001**, *183*, 3032−3040.
(3) (a) Campbell, J. W.; Cronan, J. E. *Annu. Rev. Microbiol.* **2001**, *55*, 305−332. (b) Heath, R. J.; White, S. W.; Rock, C. O. *Prog. Lipid Res.* **2001**, *40*, 467−497. (c) Zhang, Y.-M.; Marrakchi, H.; White, S. W.; Rock, C. O. *J. Lipid Res.* **2003**, *44*, 1−10. (d) Heath, R. J.; Rock, C. O. *Curr. Opin. Invest. Drugs* **2004**, *5*, 146−153. (e) Smith, S.; Witkowski, A.; Joshi, A. K. *Prog. Lipid Res.* **2003**, *42*, 289−317. (f) White, S. W.; Zheng, J.; Zhang, Y.-M.; Rock, C. O. *Annu. Rev. Biochem.* **2005**, *74*, 791−831.
(4) Matsumae, A.; Nomura, S.; Hata, T. *J. Antibiot.* **1964**, *17*, 1−7.
(5) (a) Miyakawa, S.; Suzuki, K.; Noto, T.; Harada, Y.; Okazaki, H. *J. Antibiot.* **1982**, *35*, 411−419. (b) Noto, T.; Miyakawa, S.; Oishi, H.; Endo, H.; Okazaki, H. *J. Antibiot.* **1982**, *35*, 401−410. (c) Oishi, H.; Noto, T.; Sasaki, H.; Suzuki, K.; Hayashi, T.; Okazaki, H.; Ando, K.; Sawada, M. *J. Antibiot.* **1982**, *35*, 391−395.
(6) Kodali, S.; et al. *J. Biol. Chem.* **2005**, *280*, 1669−1677.
(7) Young, K.; et al. *Antimicrob. Agents Chemother.* **2006**, *50*, 519−526.
(8) Wang, J.; et al. *Nature* **2006**, *441*, 358−361.

10.1021/ja062232p CCC: $33.50

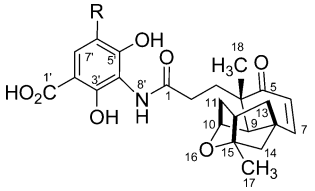

1a: R = H (Platensimycin)
1b: R = Br

Figure 1. Molecular structure of platensimycin (**1a**) and 6′-bromo derivative (**1b**).

involves specific binding with the acyl enzyme intermediate of the key condensing enzyme FabF.[8] The isolation, structure elucidation, absolute stereochemical assignment (by spectroscopic methods and X-ray crystallography of a bromo derivative (**1b**)), synthesis, and biological activity of 6,7-dihydroplatensimycin are herein described.

Results and Discussion

Platensimycin (**1a**) was isolated (2−4 mg/L) from fermentation broth of *S. platensis* (MA7327 and MA7331) originally by a three-step isolation method using Amberchrome, Sephadex LH20, and reversed-phase HPLC chromatographies. The method was modified to a two-step process, eliminating the Sephadex LH20 step. HRESIFTMS analysis afforded a molecular formula of $C_{24}H_{27}NO_7$ that was corroborated by the ^{13}C NMR spectrum in C_5D_5N and DMSO-d_6 (Table 1). The UV spectrum of **1a** displayed three absorption bands at λ_{max} 227, 240 (sh) and 296 nM. The IR spectrum indicated the presence of hydroxy (3400 cm^{-1}), ketone (1713 cm^{-1}), and benzoic acid (1650 cm^{-1}) groups. ^1H (500 MHz) and ^{13}C NMR (125 MHz) analysis of **1a** in DMSO-d_6 and C_5D_5N in combination with HMQC and DEPT spectrum provided evidence for the presence of two angular methyls, five methylenes, seven methines including four olefinic/aromatic and an oxymethine, and 10 nonprotonated carbons including a ketone, two carbonyls of carboxyl or amide types, an oxygen bearing quaternary sp^3 carbon, and two deshielded oxygen-bearing olefinic carbons. The structure of platensimycin consists of pentacyclic ketolide (right side) and 3-amino-2,4-dihydroxybenzoic acid (left side) units connected by an amide bond. A combination of DQ-COSY and TOCSY correlations led to four contiguous fragments consisting of two methylenes (C2−C3), an isolated *cis*-olefin (C6−C7), C9−C13, and an ortho-coupled aromatic (C6′−C7′). The presence of a number of quaternary carbons along with overlap of various aliphatic proton signals in the ^1H NMR spectra presented a significant challenge in structure elucidation. These problems were resolved by differential ^1H NMR analyses in DMSO-d_6 and C_5D_5N solvents. The latter solvent caused significant shifts due to anisotropic effects particularly for protons present around oxygen substituents (Table 1). Both solvents produced similar HMBC ($^nJ_{XH} = 5$ and 7 Hz) correlations except for correlations of H-10, NH, and 5′-OH, which were key in delineating the final structure. Aromatic protons H-6′ and H-7′ showed three-bond HMBC correlations to C-2′ and C-4′ and to C-3′ and C-5′, respectively. The downfield shifts of C-3′ and C-5′ indicated that they possess oxygen substitution, which was further supported by the upfield shifts of the *ortho*-carbons C-2′, C-4′, and C-6′. This was supported by HMBC correlations of 5′-OH to C-4′ and C-6′; and 8′-NH to C-3′, C-4′, and C-5′ in DMSO-d_6. The location of the carboxyl group at C-2′ was confirmed by its HMBC correlation to H-7′, thus establishing the aminobenzoic acid unit of the structure.

The structure of the more complex unprecedented ketolide unit was similarly elucidated by extensive analyses of HMBC correlations in both solvents (Table 1). The structure of the cyclohexenone ring was assembled from the HMBC correlations of the angular methyl protons (H_3-18) along with H-6 and H-7: H_3-18 exhibited strong HMBC correlations to C-4, C-5, and C-9; H-7 to C-5 and C-9; and H-6 to C-8. The HMBC correlations of H_3-18 to C-3; and H_2-3 to C-1 and C-9 helped in establishing the connectivity of C-3 to C-4 and thus the C1−C3 unit to the cyclohexenone ring. H-9 produced HMBC correlations to C-4, C-8, C-10, C-11, C-13, and C-14 which, when combined with the similar correlations of H-12 to C-8 and C-10; of H-13 to C-9, C-14, and C-15; and of H_3-17 to C-12, C-14, and C-15, established the major portion of the ketolide unit of structure **1a** except for the ether linkage. Finally, HMBC correlations of H-10 (only in C_5D_5N) to C-8, C-12, and C-15 unambiguously established the ether linkage and completed the pentacyclic ring system. An HMBC correlation of the NH to the C-1 carbonyl allowed connection of the two pieces together. This was supported by a fragment ion in ESIMS at *m*/*z* 273 due to cleavage of the amide bond (Figure 2).

The relative stereochemistry of the ketolide was elucidated by NOESY, NOEDS, and scalar couplings (Table 1). The H_3-18 axial methyl produced strong NOESY correlations (Figure 3) to the axial H-11; H-9 showed correlations to the axial H-14; and H-7 showed correlations to the equatorial H-13 and H-14, thus placing the methyl and H-11 axial on the β-face and H-9 and H-14 axial on the α-face of the molecule (Figure 3). The H-9 and H-10 signals displayed only a very small coupling (J = <1 Hz) which was consistent with the observed dihedral angle of ∼75−80° in a 3D minimized model (ChemDraw 3D).

Finally, the structure and absolute stereochemistry of **1a** were deduced by X-ray crystallographic analysis of a 6′-bromo derivative (**1b**) which was exclusively prepared by a reaction of platensimycin with 1.1 equiv of *N*-bromosuccinimide in a mixture of acetone and THF. The product was crystallized from MeOH−H_2O, and X-ray data was collected. An ORTEP drawing is represented in Figure 4. This allowed determination of absolute stereochemistry of the pentacyclic ketolide (a *trans*-cyclohexenone-pyran with 1,3,5-triaxial methylene substituents forming a fused cyclohexyl-cyclopentyl-furan) as 4*S*, 8*S*, 9*R*, 10*S*, 12*S*, and 15*S*.

Catalytic hydrogenation (with 5% Pd/C) of **1a** produced 6,7-dihydroplatensimycin **2** in quantitative yield. In acidic (0.1% TFA) aqueous CH_3CN, the keto form (**2**) slowly converts to enol form (**3**) reaching approximately 1:1 equilibrium in about 4 to 5 days. Both keto and enol forms were purified by HPLC and characterized. The enol form exists in two major conformations in a ratio of ∼2:1. No tautomerism was observed in organic solvents (e.g., methanol, pyridine). Chelating properties of *ortho*-hydroxybenzoic acid with bivalent metals tend to lower recovery of the dihydro product after reaction particularly when larger amount of catalyst was used. This phenomenon was consistent with the observation of significant binding of platensimycin to magnesium sulfate causing almost complete loss of material when magnesium sulfate was used as a drying agent for solvents. No problem was observed with sodium sulfate. The biological activities of the dihydro derivative **2** were within 4−5-fold (FabF

Table 1. ^{1}H and ^{13}C NMR Assignments of Platensimycin (**1a**) in C_5D_5N and DMSO-d_6

	C_5D_5N				DMSO-d_6		
No.	δ_C	type	δ_H (mult, J in Hz)	HMBC[a] (C → H)	δ_C	δ_H (mult, J in Hz)	$\Delta\delta_H$ (C_5D_5N-DMSO-d_6)
1	175.0	C°		H-3, NH	171.6		
2	32.4	CH_2	2.83, ddd, 14.5, 11.5, 5.5	H-3	30.3	2.03, m	+0.80
			2.75, ddd, 14.5, 11.5, 5			2.35, m	+0.40
3	32.8	CH_2	2.0, m	H-18	31.1	1.66, m	+0.34
			2.68, m			2.06, m	+0.62
4	47.4	C°		H-9, 18	45.8		
5	203.8	C°		H-7, 9, 18	202.9		
6	127.9	CH	5.94, d, 10		126.5	5.83, d, 10	+0.11
7	154.6	CH	6.37, d, 10		154.4	6.67, d, 10	−0.30
8	46.8	C°		H-6, 9, 10, 12	45.6		
9	47.2	CH	2.45, br s	H-3, 7, 13, 18	45.7	2.27, br s	+0.18
10	77.1	CH	4.49, t, 3.5	H-9, 12	75.5	4.38, br s	+0.11
11	41.4	CH_2	1.81, br d, 11.5 (ax)	H-9	40.4	1.90, m	−0.09
			1.90, m (eq)			1.98, m	−0.08
12	45.7	CH	2.20, t, 6.5	H-10, 17	44.2	2.34, m	−0.14
13	43.7	CH_2	1.57, dd, 11.5, 6.5 (eq)	H-9	42.3	1.78, dd, 11, 6.5	−0.21
			1.81, br d, 11.5 (ax)			1.94, br s	−0.13
14	55.6	CH_2	1.48, d, 11 (eq)	H-7, 13, 17	54.2	1.70, br s	−0.22
			1.73, dd, 10.5, 3 (ax)				+0.03
15	87.5	C°		H-10, 11, 13, 17	86.3		
17	23.9	CH_3	1.40, s	H-12	22.9	1.36, s	+0.04
18	25.1	CH_3	1.14, s	H-9	24.2	1.15, s	−0.01
1′	175.2	C°		H-′	172.2		
2′	107.8	C°		H-6′	104.4		
3′	158.5	C°		H-7′, NH	158.9		
4′	115.9	C°		H-6′, NH	112.8		
5′	159.1	C°		H-6′, 7′, NH	159.2		
6′	110.5	CH	6.87, d, 9		107.8	6.42, d, 9	+0.45
7′	130.1	CH	8.12, d, 9		128.9	7.54, d, 9	+0.58
8′-NH			10.5, s			9.0, s	
3′-OH						11.8, br s	
5′-OH						10.1, s	

[a] HMBC correlations in DMSO-d_6 were essentially similar to those of C_5D_5N except that the 5′-OH exhibited correlations to C-4′ and C-6′, ax (axial), eq (equatorial). W-coupling between H-14 axial and H-13 axial protons in C_5D_5N was observed.

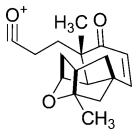

Figure 2. Structure of key mass spectral fragment ion of platensimycin.

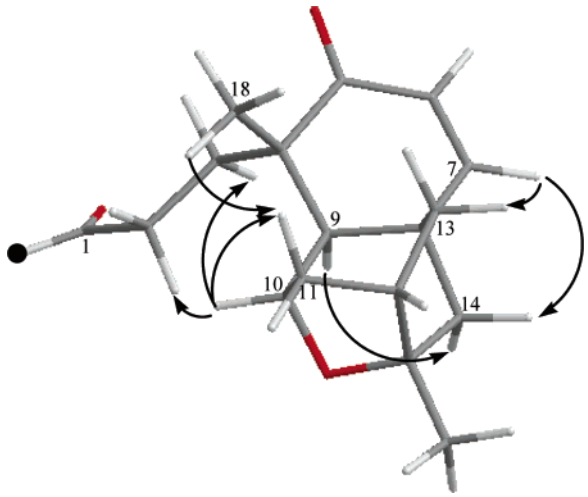

Figure 3. ChemDraw 3D model and key NOESY correlations of platensimycin; only the ketolide portion is shown.

assay in FASII format[6] IC_{50} 2 μg/mL; *S. aureus* MIC 2 μg/mL; FabF binding IC_{50} 97 nM) of **1a** (FabF IC_{50} 0.5 μg/mL; *S. aureus* MIC 0.5 μg/mL; FabF binding IC_{50} 19 nM), suggesting that potential reactivity of the enone moiety does not play a significant role for these activities. However, the data suggest that the conformation presented by the cyclohexenone ring does play a role in the binding of this compound to the enzyme by orienting the C-5 ketone for more favorable hydrogen-bonding interaction with alanine-309 of the FabF backbone.

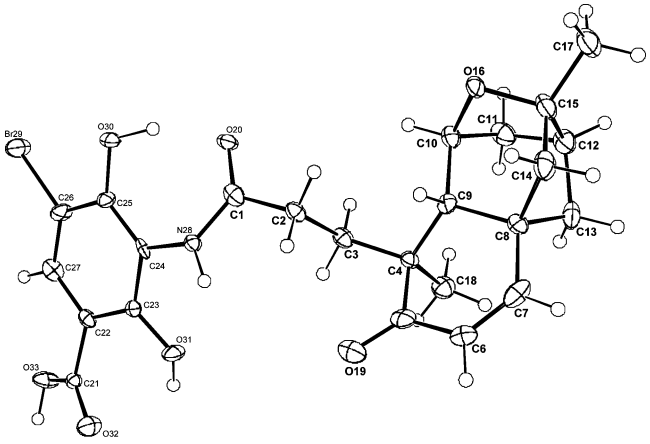

Figure 4. ORTEP drawing of crystal structure of 6′-bromo platensimycin (**1b**). Non-hydrogen atoms are represented by ellipsoids corresponding to 60% probability envelopes. Hydrogen atoms have been drawn at an arbitrary size.

In summary, we have described herein the efficient isolation, structure, and absolute stereochemistry of platensimycin, which is a novel and potent broad spectrum Gram-positive antibiotic that exerts its activity by a novel mode of action involving specific binding with the acyl enzyme intermediate of the key

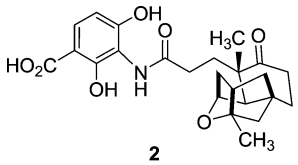

2

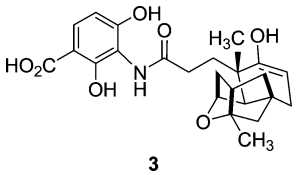

3

condensing enzyme, FabF. We have also shown that the potential reactivity of enone does not play a significant role in the biological activity; however, the conformation of the cyclohexenone ring does.

Experimental Section

General Methods. Optical rotations were measured with a Perkin-Elmer 241 polarimeter. UV spectra were recorded on a Beckman DU-70 spectrophotometer. IR spectra were recorded with a Perkin-Elmer Spectrum One FT-IR spectrophotometer. All NMR spectra were recorded with a Varian Unity 500 (^{1}H, 500 MHz, ^{13}C, 125 MHz) spectrometer. Residual protons in deuterated solvents were used as internal reference (DMSO-d_6 δ_H 2.50, δ_C 39.51; C_5D_5N δ_H 8.74, δ_C 150.35). ^{1}H−^{1}H COSY, DEPT, TOCSY, HMQC, and HMBC spectra were measured using standard Varian pulse sequences. ESIMS data were recorded on an Agilent 1100 MSD with ESI ionization. HRESIFT-MS was acquired on a Thermo Finnigan LTQ-FT with the standard Ion Max API source (without the sweep cone) and ESI probe. Three scan events were used. The ion trap was scanned from 150 to 2000 first in negative ion mode and then in positive ion mode. The FT was scanned from 200 to 2000 in the positive ion mode only. In all cases, the Source Induced Dissociation (SID) was set to 18 V to try to reduce multiple ion clusters. Instrument resolution was set to 100 000 at *m*/*z* 400. No internal calibration was required; the instrument was calibrated once a week and checked daily to ensure accuracy. An Agilent HP1100 instrument was used for analytical HPLC.

Producing Organisms. The original producing strain MA7327 was isolated from a soil sample collected in Eastern Cape, South Africa. Another producing strain MA7331 was subsequently isolated from a soil sample collected in Menorca, Balearic Islands, Spain. Both strains were identified as *S. platensis* by 16S rDNA analysis. The strains were preserved in the Merck Microbial Culture Collection with accession numbers MA7327 and MA7331.

Production of Platensimycin. The culture was maintained on agar plugs in vials containing sterile glycerol 10% stored at −80 °C until ready for use. The seed culture was inoculated by aseptically transferring four agar plugs into a 250-mL Erlenmeyer baffled flask containing 50 mL of seed medium (in g/L: soluble starch 20.0; dextrose 10.0; NZ amine type E 5.0; Difco beef extract 3.0; Difco Bacto Peptone 5.0; Difco yeast extract 5.0; and $CaCO_3$ 1.0). Seed medium was prepared with distilled water, and the pH was adjusted to 7.0 by adding NaOH before the $CaCO_3$. The flasks were capped with cellulose plugs before being autoclaved at 121 °C for 20 min. The seed culture was incubated at 28 °C on a gyratory shaker (220 rpm) for 4 days prior to the inoculation of fermentation flasks. The production medium was formulated (in g/L) as follows: Amberex pH 5.0; yellow corn meal 40.0; and lactose 40.0. The pH was adjusted to 7.0. The production medium was dispensed into 500-mL Erlenmeyer flasks (110 mL/flask) and capped with cellulose plugs before being autoclaved at 121 °C for 20 min. Fermentation flasks were inoculated with 5.5 mL of vegetative seed growth (5%) and were incubated at 28 °C, 70% humidity on a gyratory shaker (220 rpm) for 7 days before harvesting.

Isolation of Platensimycin (1a). Three liters of harvested whole broth (pH 5.5) including mycelia was extracted with 1 L of methanol by shaking for 30 min at a rotatory shaker and filtered. Mycelia were washed with 400 mL of methanol and filtered. Combined filtrate was diluted with 1 L of water and charged at a flow rate of 10 mL/min on to a 100-cm^3 Amberchrome CG161 resin column. The column was eluted with a 145-min linear gradient of 5−100% methanol at a flow rate of 10 mL/min. Fractions eluting with 70−100% aqueous methanol contained platensimycin. Pooled fractions were concentrated to dryness to afford a 90-mg residue that was chromatographed on a reversed-phase Water's Symmetry C_{18} (19 × 300 mm) column eluting with 40% aqueous CH_3CN containing 0.1% TFA. Fractions eluting at 13−14 min were pooled and lyophilized to afford 7.4 mg (2.5 mg/L) of a buff powder of platensimycin (**1a**) and crystallized from nitromethane as buff colored prisms. Mp 220−222 °C, $[\alpha]^{23}_D$ −51.1° (*c* 0.135, CH_3-OH); UV (CH_3OH) λ_{max} 227 (ϵ 28 167), 240 (sh), 296 (4825) nm, FTIR (ZnSe) ν_{max} 3400, 2964, 1713 (w), 1650 (br, strong), 1535, 1446, 1378, 1296, 1240, 1153, 1105, 1091, 1024, 953, 828, 791, 608 cm^{-1}. For ^{1}H and ^{13}C NMR assignments, see Table 1. ESIMS (*m*/*z*) 442 (M + H), 440 (M − H), 273 (M − anilide); HRESIFTMS (*m*/*z*) 442.1853 (calcd for $C_{24}H_{27}NO_7$ + H: 442.1866).

6′-Bromoplatensimycin (1b). To a solution of platensimycin (100 mg, 0.23 mmol) in acetone (0.9 mL) and THF (0.25 mL) was added *N*-bromosuccinimide (44.4 mg, 0.25 mmol) and stirred at room temperature for 2.5 h to yield bromoplatensimycin quantitatively (by HPLC). Solvents were removed, and the residue was stored at room temperature over a weekend, leading to the formation of crystals that were collected (52 mg of **1b**). Crystals were washed with 0.6 mL of methanol. The methanol soluble portion was purified by preparative reversed-phase HPLC using Zorbax RX C_8 (21 × 250 mm) column with a 37 min linear gradient of 5−95% aqueous acetonitrile (+0.1% TFA) at a flow rate of 12 mL/min. The fractions eluting at 24−28 min were combined and lyophilized to give 42 mg (combined isolated yield 84.8%) of 6′-bromoplatensimycin (**1b**). Mp 219−221 °C (dec); ^{1}H NMR (C_5D_5N) δ 1.31 (3H, s), 1.41 (3H, s), 1.50 (1H, d, J = 11 Hz), 1.59 (1H, dd, J = 11, 6.5 Hz), 1.71 (1H, dd, J = 11, 3 Hz), 1.81 (1H, d, J = 11.5 Hz), 1.82 (1H, m), 1.90−199 (2H, m), 2.22 (1H, t, J = 6 Hz), 2.39 (1H, br s), 2.57−2.78 (2H, m), 4.42 (1H, br s), 5.93 (1H, d, J = 10.5 Hz), 6.38 (1H, d, J = 10.5 Hz), 8.44 (1H, s), 10.66 (1H, s, NH), 13.32 (3H, br s); ^{13}C NMR (C_5D_5N) δ 23.8, 24.9, 32.2, 32.5, 41.3, 43.6, 45.6, 46.7, 47.1, 47.2, 55.5, 77.0, 87.4, 102.9, 109.6, 116.8, 127.7, 132.6, 154.6, 154.9, 158.0, 174.4, 175.5, 203.7; ESIMS (*m*/*z*) 522, 520 (M + H), 273 (M − anilide); HRESIFTMS (*m*/*z*) 520.0962 (calcd for $C_{24}H_{26}NO_7Br$ + H: 520.0970).

6,7-Dihydroplatensimycin (2). To a solution of platensimycin (100 mg) in methanol (3 mL) was added 5% Pd/C (10 mg) and hydrogenated using a balloon filled with hydrogen. After 4 h, catalyst was removed by filtration via a 0.45-μm PTFE filter. The filtrate was concentrated to dryness and lyophilized to produce 100 mg (100%) of **2** as a colorless amorphous powder. UV (CH_3CN-H_2O) 225, 255, 300 nm; ^{1}H NMR ($CDCl_3/CD_3OD$, 3:1) δ 1.20 (3H, s), 1.34 (3H, s), 1.39 (1H, d, J = 11.5 Hz), 1.60 (2H, m), 1.80 (2H, m), 1.95−2.09 (2H, m), 2.23 (1H, dd, J = 5, 3 Hz), 2.26 (1H, dd, J = 4.5, 3 Hz), 2.30 (1H, m), 2.41 (2H, m), 2.58 (1H, dt, J = 6, 14 Hz), 4.31 (1H, br s), 6.42 (1H, d, J = 9 Hz), 7.54 (1H, d, J = 9 Hz); ^{13}C NMR ($CDCl_3/CD_3OD$, 3:1) δ 22.5, 23.2, 31.8, 33.3, 33.9, 36.0, 40.2, 42.2, 44.1, 44.5, 49.3, 49.9, 54.8, 76.9, 86.5, 104.6, 110.1, 113.7, 128.2, 154.62, 154.66, 172.1, 174.0, 215.7; ESIMS (*m*/*z*) 444 (M + H), 442 (M − H), 275 (M − anilide); HRESIFTMS (*m*/*z*) 444.2015 (calcd for $C_{24}H_{29}NO_7$ + H: 444.2022).

A small portion (52 mg) of the keto form (**2**) was stored in 20 mL of aqueous CH_3CN +0.1% TFA for 6 days and was purified by preparative reversed-phase HPLC using Zorbax RX C_8 (21.1 × 250 mm) column eluting with a 39 min gradient of 10−90% aqueous CH_3-CN +0.1% TFA at a flow rate of 12 mL/min. The fractions eluting at 21−22 min were lyophilized immediately upon elution, yielding 26 mg of the enol form **3** as amorphous powder. The keto form **2** (11 mg) eluted at 24 min. (**3**) ^{1}H NMR (C_5D_5N) δ 1.24, 2.04 (2H, m, H_2-13), 1.30, 1.80 (2H, m, H_2-3), 1.42 (3H, s, H_3-17), 1.43, 1.67 (2H, m, H_2-14), 1.56, 1.58 (3H, s, H_3-18), 1.87, 2.27 (2H, m, H_2-7), 1.96, 2.18 (2H, m, H_2-11), 1.97 (1H, m, H-9), 2.19 (1H, m, H-12), 2.64, 2.83 (2H, m, H_2-2), 4.50, 4.55 (1H, br s, H-10), 5.11, 5.16 (1H, t, J = 4.0 Hz, H-6), 6.88, 6.93 (1H, d, J = 9 Hz, H-6′), 8.23 (1H, d, J = 9 Hz,

H-7′); ^{13}C NMR (C_5D_5N) δ 22.70, 22.79 (C-18), 23.9 (C-17), 30.28, 30.32 (C-2), 34.01 (C-7), 34.08, 34.36 (C-3), 34.82, 34.85 (C-4), 41.32 (C-11), 42.05, 42.06 (C-8), 44.85, 44.97 (C-13), 46.86 (C-12), 53.21, 53.35 (C-9), 57.71, 57.76 (C-14), 77.63, 77.67 (C-10), 86.10 (C-15), 103.90, 104.55 (C-5), 107.90, 108.09 (C-2′), 108.76, 108.88 (C-6′), 116.68, 116.80 (C-4′), 131.92 (C-7′), 142.84, 142.87 (C-4), 161.43, 161.57 (C-3′), 162.48, 161.83 (C-5′), 167.96, 168.15 (C-2), 175.03, 175.27 (C-1′); ESIMS (*m*/*z*) 426 (M − H_2O + H), 424 (M − H_2O − H).

Supporting Information Available: Copies of HPLC and UV, ^{1}H and ^{13}C NMR spectra of platensimycin, full author list of refs 6−8, and X-ray crystallographic data, in CIF format. This material is available free of charge via the Internet at http://pubs.acs.org. The supplementary crystallographic data have also been deposited as CCDC 294273. These data can be obtained free of charge from The Cambridge Crystallographic Data Centre via www.ccdc.cam.ac.uk/data_request/cif.

JA062232P